
Can Aerial VLA Models Cooperate? Evaluating Closed-Loop Air-Ground Coordination with CARLA-AIR

Tianle Zeng¹ Yanci Wen¹ Xueang Yu² Hong Zhang^{1*}

¹Southern University of Science and Technology

²Fudan University

Abstract

Recent aerial vision-language-action (VLA) models show promising single-UAV capabilities, such as tracking moving objects and navigating to language-specified landmarks. However, it remains unclear whether these capabilities can transfer to air-ground cooperation, where a UAV and a UGV must act jointly in a shared, closed-loop physical world.

We study this question with CARLA-AIR, a single-process air-ground evaluation environment that unifies CARLA and AirSim inside one Unreal Engine runtime. By sharing the same world state, physics tick, and sensing pipeline, CARLA-AIR enables physically consistent UAV-UGV interaction and precise measurement of simulation-timestamp alignment and effective coordination latency.

Using CARLA-AIR, we evaluate representative aerial VLA and planning baselines on two complementary diagnostic tasks: moving-platform landing and occlusion-recovery escort. The results show that current aerial VLA models can often track or follow a ground partner, but struggle to convert this single-agent competence into stable cooperative behavior. State prompting provides limited benefit, and naive bidirectional interaction fails to consistently improve performance and can amplify errors for most baselines. These findings suggest that, under the tested text-based cue interfaces, zero-shot cooperative air-ground VLA requires three components beyond the current paradigm: explicit partner-state grounding, low-latency action coordination, and team-level objective alignment. Our code is available at <https://github.com/louiszengCN/CarlaAir>

1 Introduction

Air-ground cooperation is becoming an important capability for embodied intelligence in urban search-and-rescue, autonomous logistics, inspection, and intelligent transportation [1]. A UAV can provide wide-area aerial perception, while a UGV can execute ground-level actions and carry heavier payloads [2]. In principle, the two platforms are highly complementary. In practice, however, turning this complementarity into real cooperation requires agents to share state, coordinate actions, and respond to each other in a closed-loop physical world [3].

Recent aerial vision-language-action (VLA) models provide a tempting starting point. They can follow language instructions, track moving ground objects, and navigate toward visual goals from onboard observations [4–7]. These abilities resemble useful components of air-ground cooperation.

*Corresponding author: Hong Zhang. Contact email: 12531293@mail.sustech.edu.cn.

This raises a central question: can single-UAV VLA competence naturally transfer to cooperative UAV-UGV behavior?

We argue that this question remains largely unanswered. Existing air-ground datasets [8] mainly evaluate offline perception, while existing interactive simulators [9, 10] often rely on bridge-based or multi-process architectures with independent clocks. Such settings make it difficult to measure whether one agent’s signal actually improves the partner’s real-time behavior, or whether apparent gains or failures are partly caused by clock mismatch and communication delay introduced by the evaluation platform itself. A reliable evaluation of cooperative VLA requires a shared physical world, closed-loop interaction, and measurable end-to-end coordination latency.

To this end, we introduce CARLA-AIR [11], a single-process air-ground evaluation environment that unifies CARLA and AirSim inside one Unreal Engine runtime. CARLA-AIR preserves CARLA’s urban traffic simulation and AirSim’s multirotor dynamics while placing UAVs and UGVs under the same world state, physics tick, and sensing pipeline. This design enables physically consistent interaction and removes the simulation-timestamp mismatch that can arise when UAV and UGV simulators are bridged as separate processes.

Built on CARLA-AIR, we evaluate whether existing aerial VLA models can move beyond single-agent behavior toward air-ground cooperation. We design two complementary diagnostic tasks. Cooperative Moving-Platform Landing tests whether visible tracking of a ground partner can become coordinated action. Cooperative Occlusion-Recovery Escort tests whether partner-state cues can help recover visual contact after temporary occlusion. Together, the two tasks probe cooperation from both the action side and the perception side, while keeping the native aerial VLA interface unchanged.

Our results reveal a consistent gap between aerial competence and cooperation. Current aerial VLA models can often track or follow the UGV, but this ability does not reliably convert into successful cooperative behavior. Partner-state prompting brings limited and unstable gains, and naive bidirectional interaction can even amplify errors. In contrast, a state-based cooperative reference performs substantially better when explicit metric state and low-latency coordination are available. These findings suggest that single-UAV VLA competence is not cooperation: cooperative air-ground VLA requires mechanisms for partner-state modeling, cooperative observation design, partner-aware action grounding, and team-level objective alignment.

Contributions.

1. **Closed-loop evaluation runtime.** We introduce and validate CARLA-AIR, a single-process air-ground evaluation runtime that unifies CARLA and AirSim for closed-loop UAV-UGV interaction. By sharing world state, physics ticks, and sensing pipelines, CARLA-AIR enables physically consistent interaction with zero simulation-timestamp mismatch by construction. This provides a reliable basis for closed-loop evaluation of air-ground cooperation without confounding the results with simulator synchronization errors.
2. **Diagnostic evaluation suite.** We introduce two complementary diagnostic tasks, moving-platform landing and occlusion-recovery escort, together with communication protocols, baselines, a state-based cooperative reference, and metrics that separate single-UAV competence from cooperative success. Together, these components form a focused diagnostic suite for isolating cooperation failure modes rather than ranking general-purpose autonomy systems.
3. **Scientific finding.** Under zero-shot evaluation and tested text-based cue protocols, current aerial VLA models do not naturally transfer single-UAV competence to air-ground cooperation: tracking does not reliably become coordination, partner cues do not consistently become recovery behavior, and naive interaction can amplify errors for most baselines.

2 Related Work

2.1 Air-Ground Evaluation Infrastructure

Existing evaluation infrastructure cannot provide reliable end-to-end assessment of closed-loop cooperative behavior. Current efforts fall into two categories, each with fundamental limitations.

Table 1: **Representative comparison of air-ground evaluation infrastructure.** Column criteria: *Single-proc. physics* = UAV and UGV share one simulation clock and physics tick; *Closed-loop coop.* = agents interact in a live closed loop; *Urban traffic* = dynamic ground traffic; *VLA eval.* = native support for vision-language-action policy evaluation; *Latency meas.* = measurable end-to-end cooperation latency. CARLA-AIR is the only interactive platform combining all five properties.

System	Single-proc. physics	Closed-loop coop.	Urban traffic	VLA eval.	Latency meas.
<i>Interactive simulation platforms</i>					
CARLA-AIR (ours)	✓	✓	✓	✓	✓
Bridge (ROS arch.)	✗	☆	☆	✗	✗
TranSimHub [9]	✗	✓	✓	✗	✗
AirSimAG [10]	✓	☆	☆	✗	✗
SimWorld-Robotics [12]	✗	✓	✓	✓	✗
UnrealZoo [13]	✗	✗	☆	✗	✗
OmniDrones [14]	✓	✗	✗	✗	✗
gym-pybullet-drones [15]	✓	✗	✗	✗	✗
RotorS [16]	✗	✗	✗	✗	✗
<i>Dataset / offline evaluation works (included for context)</i>					
UAV3D [8]	✗	✗	✓	✗	✗
Griffin [17]	✗	✗	✓	✗	✗
OpenFly [5]	N/A	✗	✗	✓	✗
UAV-Flow [18]	N/A	✗	✗	✓	✗

✓ = Yes; ✗ = No; ☆ = Partial; N/A = not applicable.

Air-ground cooperation benchmarks. Several air-ground datasets and benchmarks study cooperation between aerial and ground agents, including UAV3D [8], CoPerception-UAVs [19], AirV2X [20], and Griffin [17]—but all evaluate perception modules (detection, tracking, feature fusion) on pre-collected datasets. Because agents do not interact in a live closed loop, these benchmarks cannot reveal whether one agent’s signal improves the partner’s real-time behavior or changes the final cooperative outcome.

Air-ground simulation platforms. Existing interactive platforms either rely on multi-process or bridge-based architectures with independent clocks, or lack the full combination of dynamic urban traffic, VLA evaluation, and latency-measurable closed-loop cooperation. The standard approach couples CARLA [21] and AirSim [22] or RotorS [16] via a ROS bridge, introducing timing jitter that corrupts latency measurement. TranSimHub [9] supports complex air-ground traffic scenarios but retains the same multi-process synchronisation limitation. Recent urban embodied AI platforms like SimWorld-Robotics [12] and UnrealZoo [13] provide rich, photo-realistic environments supporting both UAVs and ground vehicles, yet they lack the strict high-frequency physics synchronization required for precise air-ground control. AirSimAG [10] achieves single-process execution and supports basic UAV-UGV coordination, but lacks dynamic urban ground traffic and native support for evaluating VLA policies. Similarly, reinforcement learning-oriented UAV platforms such as OmniDrones [14] and gym-pybullet-drones [15] offer scalable multi-agent training for aerial tasks, but are not designed for urban traffic realism or closed-loop ground interaction. None provides the combination of a unified physical world, closed-loop interaction, and precise latency instrumentation needed to reliably evaluate air-ground cooperation. CARLA-AIR is designed to fill this gap.

2.2 Methods for Air-Ground Cooperation

Modular and task-specific approaches. Air-ground cooperation has been explored through modular and task-specific systems. [23] combine an LLM planner with metric navigation for language-specified aerial-ground missions, while cooperative perception methods such as Where2Comm [24] learn communication-efficient feature sharing across agents. Bidirectional trajectory optimization [25] couples UAV and moving-platform trajectories for agile landing, and GLIDE [26] uses compact georeferenced messages for role-separated UAV-UGV teaming in search-and-rescue. Learning-based approaches [27] further train partner-aware policies through structured observation interfaces. These works show that air-ground cooperation can be achieved with task-specific protocols, state representations, and coordination mechanisms, but their reliance on designed interfaces or task-specific coordination pipelines limits generalization to open-ended language instructions. This

motivates studying end-to-end aerial VLA models as more general language-conditioned UAV-side agents for air-ground cooperation.

End-to-end aerial VLA models. End-to-end vision-language-action models that unify perception, reasoning, and control have made rapid progress on the aerial side. Methods [5, 7] enable UAVs to navigate to ground-level landmarks from language instructions; UAV-Track VLA [4] achieves autonomous aerial tracking of moving ground vehicles; and AerialVLA [28] extends language-conditioned control to complex flight manoeuvres involving ground-scene understanding. Recent benchmarks like UAV-Flow [18] further demonstrate that aerial VLAs can perform language-guided fine-grained trajectory control in real-world flights. These models already perform tasks that closely resemble components of air-ground cooperation, making them promising candidates as the UAV-side agent in a cooperative system. However, whether their single-platform competence transfers to multi-platform cooperation has not been evaluated. CARLA-AIR provides both the platform and the diagnostic suite to conduct this evaluation.

3 CARLA-AIR Platform

To support shared-world interaction and latency-measurable closed-loop evaluation, CARLA-AIR implements a single-runtime design in which aerial and ground agents share the same world state, simulation clock, and physics tick. The key design choice is to embed CARLA and AirSim into one engine-level runtime rather than synchronizing two simulator processes after execution. This section describes how the runtime resolves simulator ownership, preserves native interfaces, and validates that the resulting measurements are free from inter-process synchronization noise.

3.1 Causally Consistent Runtime Architecture

Resolving the single-authority constraint. The main obstacle is not simply co-locating two large codebases, but reconciling two independent notions of simulation authority within one runtime world. In Unreal Engine, each simulation world has a single authoritative lifecycle controller, implemented as `GameMode` [29]. Since CARLA and AirSim were both designed as standalone backends, a naive merge would create two competing controllers over the same world state. This is why conventional integrations place the two simulators in separate processes and synchronize them externally.

CARLA-AIR resolves this conflict by exploiting an asymmetry in how the two backends depend on runtime authority. CARLA behaves as a *controller-dominant* backend: its traffic manager, weather system, episode management, sensor scheduling, and RPC services are tightly bound to the global lifecycle controller. AirSim, in contrast, is *actor-realizable*: its multicopter dynamics and flight control logic are encapsulated in an actor-level vehicle entity and do not require ownership of the global controller.

This asymmetry yields a single-authority, multi-actor runtime. CARLA-AIR preserves CARLA as the authoritative world manager and instantiates AirSim as an actor-level aerial subsystem in the same simulation world. Concretely, `CARLAAirGameMode` inherits CARLA’s native `GameMode` to retain ground-vehicle simulation, traffic, weather, episode, sensor, and RPC functionalities, while composing the AirSim flight actor as a standard world entity during engine initialization. Thus, the integration changes the runtime ownership model without reimplementing either simulator.

Shared-clock execution. Timestamp alignment follows from the runtime structure rather than from an additional synchronization module. Once the AirSim vehicle is composed as a world actor, both the UGV and UAV are advanced by the same engine scheduler. At each tick, the runtime applies ground and aerial commands, advances the shared physics state, and samples sensors from the updated world state. UAV and UGV observations are therefore generated from the same state transition, not aligned after generation. This makes matched sensor timestamps identical by construction in the single-threaded execution path.

Native interfaces under a unified runtime. CARLA-AIR changes the runtime boundary, not the user-facing API boundary. CARLA and AirSim retain their original RPC servers and client protocols, so existing ground and aerial policies can still issue commands through the standard CARLA and AirSim Python APIs. The difference is that both command streams are resolved inside the same runtime world: CARLA commands act on the authoritative ground subsystem, while AirSim com-



Figure 1: **CARLA-AIR runtime architecture.** CARLA and AirSim are embedded in one engine-level runtime with a shared world state, physics tick, and sensor/rendering pipeline. Native CARLA and AirSim APIs are preserved, while both command streams are resolved inside the same runtime.

Table 2: **Runtime consistency validation.** Across 100 matched episodes, the bridge runtime introduces non-zero UAV-UGV sensor offsets and substantially higher variance in the cooperation metric. CARLA-AIR eliminates simulation-timestamp mismatch under synchronized tick sampling and reduces measurement noise by $5.1\times$.

Metric	Bridge runtime	CARLA-AIR runtime
Mean sensor offset (ms)	12.4	0.0
Std. sensor offset (ms)	8.9	0.0
Max sensor offset (ms)	34	0.0
Std. cooperation metric	0.143	0.028
Measurement-noise reduction	$1.0\times$	$5.1\times$

mands act on the composed aerial actor. Native API compatibility is therefore preserved without reintroducing an external bridge or independent simulation clocks.

Coordinate-frame unification, sensor scheduling, synchronous rendering, API compatibility, and hardware requirements are detailed in Appendix A.

3.2 Runtime Consistency Check

Before using CARLA-AIR for cooperative VLA evaluation, we verify that platform-level synchronization noise is small relative to the cooperation effects we aim to measure. As a control, we compare CARLA-AIR against a standard ROS-bridge configuration in which CARLA and AirSim run as separate processes—the architecture used by prior air-ground integrations [3]. Both runtimes execute the same 100 matched episodes; the only varied factor is the runtime architecture. Full protocol details are in Appendix A.

As Table 2 shows, the bridge configuration introduces non-zero UAV-UGV sensor offsets (mean 12.4 ms, max 34 ms—roughly one third of a 10 Hz control cycle), whereas CARLA-AIR samples matched frames from the same simulation tick and yields $\Delta t = 0$ ms by construction. The cooperation-metric standard deviation drops correspondingly from $\sigma = 0.143$ to $\sigma = 0.028$, a $5.1\times$ reduction that places CARLA-AIR’s noise floor well below the cooperation effects reported in Section 4. Extended results across heavier sensor loads, higher control rates, and multi-agent scenarios in Appendix A show consistent $4.2\text{--}6.3\times$ noise reduction across all settings.

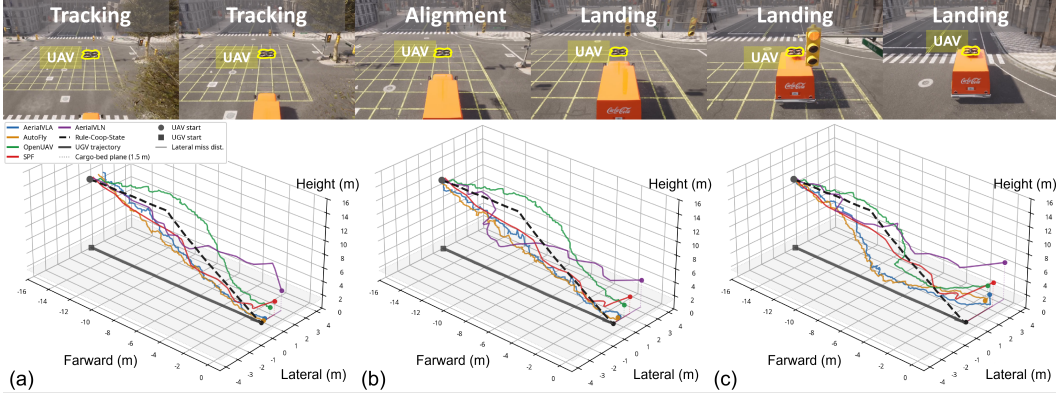


Figure 2: **Landing process trajectory diagnosis.** Top: representative visual sequence during moving-platform landing. Bottom: 3D UGV and UAV trajectories during moving-platform landing under (a) C0, (b) C1, and (c) C2. Colored curves denote aerial baselines; gray line denotes the UGV trajectory; black dashed line denotes Rule-Coop-State.

4 Diagnostic Evaluation

Building on the physically consistent and closed-loop evaluation runtime, we use CARLA-AIR to answer the central question of this paper: can existing aerial VLA models transfer their single-UAV competence to cooperative air-ground behavior?

We design two complementary diagnostic tasks. *Cooperative Moving-Platform Landing* diagnoses action-side coordination: the UAV must track a moving UGV, align with its rear cargo bed, and land safely. *Cooperative Occlusion-Recovery Escort* diagnoses perception-side recovery: the UAV must recover visual contact with a temporarily occluded UGV using partner-state cues. Both tasks keep the native aerial VLA interface unchanged: the policy receives visual observations and language instructions, and outputs only UAV actions.

4.1 Tasks and Cooperation Protocol

In Moving-Platform Landing, a UGV truck drives along an urban road while providing a flat rear cargo bed as the landing surface. The task requires the UAV to convert visible tracking into aligned descent and touchdown on a moving platform. In Occlusion-Recovery Escort, the UGV becomes temporarily occluded by bridges, buildings, or large artifacts; the UAV must use partner-state cues to re-establish visual contact after the occlusion.

We evaluate three cooperation modes. C0 uses independent execution with no communication. C1 adds a compact UGV-to-UAV partner-state cue while the UGV follows its predefined behavior. C2, used only for the landing task, additionally passes the magnitude of the UAV’s forward-velocity action signal to the UGV’s longitudinal controller, providing a naive form of bidirectional UAV-to-UGV action coupling. The signal is derived from each baseline’s native action interface (Appendix B). Escort uses only C0 and C1. Full prompt templates and controller details are provided in Appendix B.

4.2 Baselines and Metrics

Table 3 summarizes the evaluated methods, spanning end-to-end VLA, VLM-based planning, and traditional aerial VLN. Each baseline is run through its native low-level wrapper (Appendix B); reported numbers reflect policy-family characteristics rather than implementation-matched rankings.

Rule-Coop-State is included as a solvability reference, not as a fair baseline. It uses explicit metric state—UAV–cargo-bed relative pose, relative velocity, UGV speed, and landing phase—unavailable to VLA baselines, with deterministic low-latency rules. The gap between Rule-Coop-State and VLA methods therefore reflects both architectural and informational differences. We interpret all subsequent results under this framing.

Table 3: **Baseline and reference summary.**

Method	Category	Native output
<i>Zero-shot aerial policies</i>		
AerialVLA [28]	End-to-end VLA	Continuous UAV action
OpenFly [5]	End-to-end VLA	Discrete UAV action
OpenUAV [30]	End-to-end VLA	Continuous UAV action
SPF [31]	VLM + explicit planning	UAV flight waypoint
AerialVLN [7]	End-to-end VLN	Discrete UAV action
<i>State-based cooperative reference</i>		
Rule-Coop-State	Rule-based cooperation	UAV/UGV actions



Figure 3: **Cooperative Occlusion-Recovery Escort.** The UAV escorts the UGV, loses visual contact under temporary occlusion, searches using partner-state cues, and re-acquires the UGV before resuming escort.

For landing, we report Tracking Success Rate (TSR) as the single-UAV primitive score and Landing Success Rate (LSR) as the final cooperative task score. We define Cooperative Conversion Rate as $CCR = LSR / \max(TSR, \varepsilon)$ with $\varepsilon = 0.05$, and Cooperation Gain as $CG(C_k) = LSR(C_k) - LSR(C_0)$. For occlusion recovery, we report Recovery Success Rate (RSR) and Re-acquisition Time (RAT). We also report Decision Frequency (DF) and Effective Coordination Latency (ECL). Detailed metric definitions are provided in Appendix B.

4.3 Results

Moving-platform landing. Table 4 shows that VLA baselines achieve non-trivial TSR under C0, but their LSR and CCR remain much lower: tracking rarely converts into successful cooperative landing.

Adding interaction does not close this gap. Under C1, 4 of 5 baselines exhibit negative CG, but the across-baseline trend is not significant; under C2, all 5 baselines are negative, a significant trend ($p=0.188$ vs. 0.031 , sign test). At the single-baseline level, AerialVLA’s CG is statistically negative under both modes, with 95% CIs excluding zero: $CG(C1) \in [-0.07, -0.01]$ and $CG(C2) \in [-0.10, -0.04]$. Naive UAV-to-UGV action coupling under C2 thus introduces unstable cooperative dynamics rather than stabilizing the task.

Rule-Coop-State reaches LSR 0.42, indicating that the task is tractable when explicit state grounding is available. Figure 2 provides a process-level diagnosis: VLA baselines often follow the truck but fail to converge smoothly to the cargo-bed region, while C2 introduces larger oscillations and Rule-Coop-State produces a more stable descent.

Timing. Heavier planning-based methods have lower decision frequency and larger effective coordination latency, making C2 feedback harder to stabilize (Appendix B, Table 13). Yet latency alone does not explain the failure: faster methods such as AerialVLN still show poor cooperative conversion. The degradation is therefore both temporal and structural.

Prompt-format ablation. Table 6 shows a consistent pattern across both tasks: semantic, numeric, and noisy cue formats all fail to close the cooperation gap. Even oracle geometric cues (C1-Oracle-Bearing) provide only marginal LSR gains, with CGs within seed-level variability. Under this text-prompt interface, the bottleneck is action grounding rather than cue format or completeness.

Occlusion recovery. Figure 3 illustrates the occlusion-recovery escort task. Table 5 shows that VLA baselines do not consistently benefit from C1 partner-state cues; for 4 of 5 baselines, the C0 vs. C1 RSR difference is within seed-level variability. SPF shows a meaningful RSR gain (+0.08), likely because the cue (*forward-right side*) aligns with its native waypoint output space; the same

Table 4: **Main results on Cooperative Moving-Platform Landing.** C0/C1/C2: cooperation modes (Section 4.1). Ref.: state-based cooperative reference. Values are mean \pm std over 3 seeds \times 50 episodes.

Method	Mode	TSR \uparrow	LSR \uparrow	CCR \uparrow	CG \uparrow
AerialVLA	C0	0.78 \pm 0.04	0.13 \pm 0.03	0.17 \pm 0.02	0.00
AerialVLA	C1	0.76 \pm 0.04	0.10 \pm 0.03	0.13 \pm 0.02	-0.03 \pm 0.02
AerialVLA	C2	0.70 \pm 0.04	0.06 \pm 0.02	0.09 \pm 0.02	-0.07 \pm 0.02
OpenFly	C0	0.81 \pm 0.03	0.14 \pm 0.03	0.17 \pm 0.02	0.00
OpenFly	C1	0.79 \pm 0.04	0.10 \pm 0.03	0.13 \pm 0.02	-0.04 \pm 0.02
OpenFly	C2	0.73 \pm 0.04	0.05 \pm 0.02	0.07 \pm 0.02	-0.09 \pm 0.02
OpenUAV	C0	0.74 \pm 0.04	0.09 \pm 0.03	0.12 \pm 0.02	0.00
OpenUAV	C1	0.70 \pm 0.04	0.06 \pm 0.02	0.09 \pm 0.02	-0.03 \pm 0.02
OpenUAV	C2	0.64 \pm 0.04	0.03 \pm 0.02	0.05 \pm 0.02	-0.06 \pm 0.02
SPF	C0	0.62 \pm 0.04	0.06 \pm 0.02	0.10 \pm 0.02	0.00
SPF	C1	0.60 \pm 0.04	0.04 \pm 0.02	0.07 \pm 0.02	-0.02 \pm 0.02
SPF	C2	0.55 \pm 0.04	0.02 \pm 0.01	0.04 \pm 0.02	-0.04 \pm 0.02
AerialVLN	C0	0.55 \pm 0.03	0.03 \pm 0.02	0.05 \pm 0.02	0.00
AerialVLN	C1	0.51 \pm 0.03	0.02 \pm 0.01	0.04 \pm 0.01	-0.01 \pm 0.01
AerialVLN	C2	0.47 \pm 0.03	0.01 \pm 0.01	0.02 \pm 0.01	-0.02 \pm 0.01
<i>State-based cooperative reference</i>					
Rule-Coop-State	Ref.	0.84 \pm 0.03	0.42 \pm 0.03	0.50 \pm 0.03	—

Table 5: **Results on Cooperative Occlusion-Recovery Escort.** RSR: visual contact recovered (IoU \geq 0.15) within 15 s of occlusion onset. RAT: re-acquisition time (s); capped at 15 s. Ref.: state-based cooperative reference. Values are mean \pm std over 3 seeds \times 50 episodes.

Method	Mode	RSR \uparrow	RAT (s) \downarrow
AerialVLA	C0	0.56 \pm 0.04	4.8 \pm 0.3
AerialVLA	C1	0.58 \pm 0.04	4.6 \pm 0.3
OpenFly	C0	0.59 \pm 0.04	4.5 \pm 0.3
OpenFly	C1	0.57 \pm 0.04	4.7 \pm 0.3
OpenUAV	C0	0.48 \pm 0.04	6.2 \pm 0.4
OpenUAV	C1	0.44 \pm 0.04	6.7 \pm 0.4
SPF	C0	0.46 \pm 0.04	6.5 \pm 0.4
SPF	C1	0.54 \pm 0.04	5.4 \pm 0.3
AerialVLN	C0	0.41 \pm 0.03	7.2 \pm 0.4
AerialVLN	C1	0.40 \pm 0.03	7.4 \pm 0.4
<i>State-based cooperative reference</i>			
Rule-Coop-State	Ref.	0.86 \pm 0.03	1.8 \pm 0.2

cue provides no benefit in landing, where it must be decomposed into continuous descent control. Rule-Coop-State reaches RSR 0.86.

Summary diagnosis. Across both tasks, current zero-shot aerial VLA policies fail to translate partner-state cues into cooperative action: tracking does not become coordinated landing, and partner-state cues do not become recovery behavior. The failure is not in cue design or cue completeness: across-baseline statistical evidence, prompt-format ablations, and oracle bearing cues all converge on the same attribution—the missing mechanism is partner-aware action grounding within the autoregressive text-prompt interface itself. Rule-Coop-State, with explicit metric state and rule-based coordination, substantially outperforms VLA baselines on both tasks, marking the gap as architectural rather than fundamental to the cooperation problem.

Table 6: **Prompt-format ablation (landing and escort)**. Cue variants: C1-Sem (default semantic), C1-Num (structured numeric), C1-Noisy (corrupted), C1-Oracle-Bearing (ground-truth range / azimuth / elevation). Values are mean \pm std over 3 seeds \times 50 episodes. Full prompt templates in Appendix B.

Method	Setting	LSR \uparrow	CCR \uparrow	CG \uparrow	RSR \uparrow	RAT \downarrow
AerialVLA	C0	0.13 \pm 0.03	0.17 \pm 0.02	0.00	0.56 \pm 0.04	4.8 \pm 0.3
AerialVLA	C1-Sem	0.10 \pm 0.03	0.13 \pm 0.02	-0.03 \pm 0.02	0.58 \pm 0.04	4.6 \pm 0.3
AerialVLA	C1-Num	0.08 \pm 0.02	0.11 \pm 0.02	-0.05 \pm 0.02	0.52 \pm 0.04	5.2 \pm 0.3
AerialVLA	C1-Noisy	0.05 \pm 0.02	0.07 \pm 0.02	-0.08 \pm 0.02	0.43 \pm 0.04	6.4 \pm 0.4
AerialVLA	C1-Oracle-Bearing	0.14 \pm 0.03	0.18 \pm 0.02	+0.01 \pm 0.02	0.62 \pm 0.04	4.3 \pm 0.3
OpenFly	C0	0.14 \pm 0.03	0.17 \pm 0.02	0.00	0.59 \pm 0.04	4.5 \pm 0.3
OpenFly	C1-Sem	0.10 \pm 0.03	0.13 \pm 0.02	-0.04 \pm 0.02	0.57 \pm 0.04	4.7 \pm 0.3
OpenFly	C1-Num	0.07 \pm 0.02	0.09 \pm 0.02	-0.07 \pm 0.02	0.50 \pm 0.04	5.5 \pm 0.3
OpenFly	C1-Noisy	0.04 \pm 0.02	0.06 \pm 0.02	-0.10 \pm 0.02	0.41 \pm 0.04	6.8 \pm 0.4
OpenFly	C1-Oracle-Bearing	0.13 \pm 0.03	0.16 \pm 0.02	-0.01 \pm 0.02	0.61 \pm 0.04	4.4 \pm 0.3

5 Discussion and Conclusion

Interaction is not cooperation. Adding cross-agent information does not automatically produce cooperation. C1 and C2 provide more partner state and action feedback, yet performance can degrade. The missing component is not information, but a mechanism that maps partner state into the model’s own action for a shared task.

Timing amplifies the failure. Larger effective coordination latency makes bidirectional feedback harder to stabilize, but latency alone does not explain the failure: faster aerial VLAs still show poor cooperative conversion, suggesting that the degradation is structural rather than purely temporal.

Implications. Cooperative VLA likely requires explicit partner-state modeling, shared task-phase representation, team-level objectives, and low-latency coordination modules.

Limitations. Our study has five principal boundaries: (i) simulation only; (ii) the cooperative burden falls primarily on the UAV side, with UGV-side cooperative planning unstudied; (iii) information asymmetry between Rule-Coop-State and VLA baselines; (iv) zero-shot VLA evaluation without cooperation-aware fine-tuning; (v) a limited set of occlusion types, with learned cooperation policies and non-VLA baselines left for future work. The sim-to-real effect remains empirically open.

Broader impact. CARLA-AIR could be repurposed for aerial tracking or surveillance, and safety-critical or privacy-sensitive deployments require independent ethical review. Our results caution against deploying zero-shot aerial VLA systems in cooperative scenarios with moving ground partners without cooperation-aware design and closed-loop validation.

Conclusion. We presented CARLA-AIR, a single-process air-ground evaluation environment for closed-loop UAV-UGV cooperation, and used it to diagnose whether single-UAV aerial VLA competence transfers to cooperative air-ground behavior. Across moving-platform landing and occlusion-recovery escort, current zero-shot aerial VLA models can track or follow a ground partner but fail to convert this ability into stable cooperation: partner-state prompting helps inconsistently, and naive bidirectional interaction can amplify errors. Prompt-format ablations and oracle-bearing cues show that the bottleneck is not cue design but partner-state grounding into action within a text-prompt interface.

References

- [1] Runqi Chai, Yunlong Guo, Zongyu Zuo, Kaiyuan Chen, Hyo-Sang Shin, and Antonios Tsourdos. Cooperative motion planning and control for aerial-ground autonomous systems: Methods and applications. *Progress in Aerospace Sciences*, 146:101005, 2024.
- [2] Tianle Zeng, Jianwei Peng, Hanjing Ye, Guangcheng Chen, Senzi Luo, and Hong Zhang. Ezreal: Enhancing zero-shot outdoor robot navigation toward distant targets under varying visibility. *arXiv preprint arXiv:2509.13720*, 2025.

- [3] Hanxuan Chen, Jie Zheng, Siqi Yang, Tianle Zeng, Siwei Feng, Songsheng Cheng, Ruilong Ren, Hanzhong Guo, Shuai Yuan, Xiangyue Wang, et al. Vision-and-language navigation for uavs: Progress, challenges, and a research roadmap. *arXiv preprint arXiv:2604.13654*, 2026.
- [4] Qiyao Zhang, Shuhua Zheng, Jianli Sun, Chengxiang Li, Xianke Wu, Zihan Song, Zhiyong Cui, Yisheng Lv, and Yonglin Tian. Uav-track vla: Embodied aerial tracking via vision-language-action models. *arXiv preprint arXiv:2604.02241*, 2026.
- [5] Yunpeng Gao, Chenhui Li, Zhongrui You, Junli Liu, Zhen Li, Peng Chen, Qizhi Chen, Zhonghan Tang, Liansheng Wang, Penghui Yang, et al. Openfly: A comprehensive platform for aerial vision-language navigation. *arXiv preprint arXiv:2502.18041*, 2025.
- [6] Oleg Sautenkov, Yasheerah Yaqoot, Artem Lykov, Muhammad Ahsan Mustafa, Grik Tadevosyan, Aibek Akhmetkazy, Miguel Altamirano Cabrera, Mikhail Martynov, Sausar Karaf, and Dzmitry Tsetserukou. Uav-vla: Vision-language-action system for large scale aerial mission generation. In *2025 20th ACM/IEEE International Conference on Human-Robot Interaction (HRI)*, pages 1588–1592. IEEE, 2025.
- [7] Shubo Liu, Hongsheng Zhang, Yuankai Qi, Peng Wang, Yanning Zhang, and Qi Wu. Aerialvln: Vision-and-language navigation for uavs. In *Proceedings of the IEEE/CVF International Conference on Computer Vision*, pages 15384–15394, 2023.
- [8] Hui Ye, Rajshekhar Sunderraman, and Shihao Ji. Uav3d: A large-scale 3d perception benchmark for unmanned aerial vehicles. *Advances in Neural Information Processing Systems*, 37: 55425–55442, 2024.
- [9] Maonan Wang, Yirong Chen, Yuxin Cai, Aoyu Pang, Yuejiao Xie, Zian Ma, Chengcheng Xu, Kemou Jiang, Ding Wang, Laurent Roullet, et al. Transimhub: A unified air-ground simulation platform for multi-modal perception and decision-making. *arXiv preprint arXiv:2510.15365*, 2025.
- [10] Yangjie Cui, Xin Dong, Boyang Gao, Jinwu Xiang, Daochun Li, and Zhan Tu. Airsimag: A high-fidelity simulation platform for air-ground collaborative robotics. *arXiv preprint arXiv:2603.23079*, 2026.
- [11] Tianle Zeng, Yanci Wen, and Hong Zhang. Carla-air: Fly drones inside a carla world—a unified infrastructure for air-ground embodied intelligence. *arXiv preprint arXiv:2603.28032*, 2026.
- [12] Yan Zhuang, Jiawei Ren, Xiaokang Ye, Jianzhi Shen, Ruixuan Zhang, Tianai Yue, Muhammad Faayez, Xuhong He, Ziqiao Ma, Lianhui Qin, et al. Simworld-robotics: Synthesizing photo-realistic and dynamic urban environments for multimodal robot navigation and collaboration. *arXiv preprint arXiv:2512.10046*, 2025.
- [13] Fangwei Zhong, Kui Wu, Churan Wang, Hao Chen, Hai Ci, Zhoujun Li, and Yizhou Wang. Unrealzoo: Enriching photo-realistic virtual worlds for embodied ai. In *Proceedings of the IEEE/CVF International Conference on Computer Vision*, pages 5769–5779, 2025.
- [14] Botian Xu, Feng Gao, Chao Yu, Ruize Zhang, Yi Wu, and Yu Wang. Omnidrones: An efficient and flexible platform for reinforcement learning in drone control. *IEEE Robotics and Automation Letters*, 9(3):2838–2844, 2024.
- [15] Jacopo Panerati, Hehui Zheng, SiQi Zhou, James Xu, Amanda Prorok, and Angela P Schoellig. Learning to fly—a gym environment with pybullet physics for reinforcement learning of multi-agent quadcopter control. In *2021 IEEE/RSJ International Conference on Intelligent Robots and Systems (IROS)*, pages 7512–7519. IEEE, 2021.
- [16] Fadri Furrer, Michael Burri, Markus Achtelik, and Roland Siegwart. Rotors—a modular gazebo mav simulator framework. In *Robot Operating System (ROS) The Complete Reference (Volume 1)*, pages 595–625. Springer, 2016.
- [17] Jiahao Wang, Xiangyu Cao, Jiaru Zhong, Yun'er Zhang, Zeyu Han, Haibao Yu, Chuang Zhang, Lei He, Shaobing Xu, and Jianqiang Wang. Griffin: Aerial-ground cooperative detection and tracking dataset and benchmark. In *Proceedings of the AAAI Conference on Artificial Intelligence*, volume 40, pages 9867–9875, 2026.

- [18] Xiangyu Wang, Donglin Yang, Yue Liao, Wenhao Zheng, Wenjun Wu, Bin Dai, Hongsheng Li, and Si Liu. Uav-flow colosso: A real-world benchmark for flying-on-a-word uav imitation learning. *arXiv preprint arXiv:2505.15725*, 2025.
- [19] Yiming Li, Juexiao Zhang, Dekun Ma, Yue Wang, and Chen Feng. Multi-robot scene completion: Towards task-agnostic collaborative perception. In *Conference on Robot Learning*, pages 2062–2072. PMLR, 2023.
- [20] Xiangbo Gao, Yuheng Wu, Fengze Yang, Xuewen Luo, Keshu Wu, Xinghao Chen, Yuping Wang, Chenxi Liu, Yang Zhou, and Zhengzhong Tu. Airv2x: Unified air-ground vehicle-to-everything collaboration. *arXiv preprint arXiv:2506.19283*, 2025.
- [21] Alexey Dosovitskiy, German Ros, Felipe Codevilla, Antonio Lopez, and Vladlen Koltun. CARLA: An open urban driving simulator. In *Proceedings of the 1st Conference on Robot Learning (CoRL)*, pages 1–16. PMLR, 2017.
- [22] Shital Shah, Debadeepta Dey, Chris Lovett, and Ashish Kapoor. AirSim: High-fidelity visual and physical simulation for autonomous vehicles. In *Field and Service Robotics (FSR)*, pages 621–635. Springer, 2018.
- [23] Fernando Cladera, Zachary Ravichandran, Jason Hughes, Varun Murali, Carlos Nieto-Granda, M Ani Hsieh, George J Pappas, Camillo J Taylor, and Vijay Kumar. Air-ground collaboration for language-specified missions in unknown environments. *IEEE Transactions on Field Robotics*, 2025.
- [24] Yue Hu, Shaoheng Fang, Zixing Lei, Yiqi Zhong, and Siheng Chen. Where2comm: Communication-efficient collaborative perception via spatial confidence maps. *Advances in neural information processing systems*, 35:4874–4886, 2022.
- [25] Chunhui Zhao, Xirui Kao, Yilin Lu, and Yang Lyu. A bi-directional adaptive framework for agile uav landing. *arXiv preprint arXiv:2601.03037*, 2026.
- [26] Seth Farrell, Chenghao Li, Hongzhan Yu, Hesam Mojtahedi, Sicun Gao, and Henrik I Christensen. Glide: A coordinated aerial-ground framework for search and rescue in unknown environments. *arXiv preprint arXiv:2509.14210*, 2025.
- [27] Enguang Fan, Yifan Chen, Zihan Shan, Matthew Caesar, and Jae Kim. Communication-aware multi-agent reinforcement learning for decentralized cooperative uav deployment. *arXiv preprint arXiv:2603.16141*, 2026.
- [28] Peng Xu, Zhengnan Deng, Jiayan Deng, Zonghua Gu, and Shaohua Wan. Aerialvla: A vision-language-action model for uav navigation via minimalist end-to-end control. *arXiv preprint arXiv:2603.14363*, 2026.
- [29] Oleksandra Sobchysyak, Santiago Berrezueta-Guzman, and Stefan Wagner. Pushing the boundaries of immersion and storytelling: A technical review of unreal engine. *Displays*, page 103268, 2025.
- [30] Xiangyu Wang, Donglin Yang, Ziqin Wang, Hohin Kwan, Jinyu Chen, Wenjun Wu, Hongsheng Li, Yue Liao, and Si Liu. Towards realistic uav vision-language navigation: Platform, benchmark, and methodology. *arXiv preprint arXiv:2410.07087*, 2024.
- [31] Chih Yao Hu, Yang-Sen Lin, Yuna Lee, Chih-Hai Su, Jie-Ying Lee, Shr-Ruei Tsai, Chin-Yang Lin, Kuan-Wen Chen, Tsung-Wei Ke, and Yu-Lun Liu. See, point, fly: A learning-free vlm framework for universal unmanned aerial navigation. In *Conference on Robot Learning*, pages 4697–4708. PMLR, 2025.
- [32] CodexLabsLLC. Colosseum: An open-source simulator for autonomous robotics research. <https://github.com/CodexLabsLLC/Colosseum>, 2024. Community fork of AirSim.

Appendix

This appendix provides additional platform and evaluation details that support the main paper. Appendix A describes the CARLA-AIR runtime design, coordinate-frame unification, sensing support, software stack, and runtime consistency validation. Appendix B provides task settings, cooperation modes, prompt templates, metric definitions, baseline adaptations, and timing statistics.

A CARLA-AIR Platform Details

This appendix provides implementation details for CARLA-AIR, including coordinate-frame unification, sensor and API support, software versions, source modifications, and runtime requirements. Figure 4 illustrates the core integration mechanism: CARLA-AIR resolves the single-GameMode constraint by keeping CARLA as the authoritative world manager and composing the AirSim aerial subsystem as an actor-level component.

A.1 Coordinate Frame Unification and Single-Tick Execution

All cross-agent states, observations, and cooperation metrics are expressed in a unified metric frame. CARLA uses a left-handed Unreal Engine frame (centimetres, Z -up), while AirSim adopts a NED frame (metres, Z -down). As illustrated in Figure 5, we apply a deterministic transformation at every simulation tick:

$$\mathbf{P}_{\text{NED}} = \frac{1}{100} \begin{pmatrix} p_x - o_x \\ p_y - o_y \\ -(p_z - o_z) \end{pmatrix}, \quad q_{\text{NED}} = \frac{(w, q_x, q_y, -q_z)}{\|(w, q_x, q_y, -q_z)\|}, \quad (1)$$

where (o_x, o_y, o_z) is the AirSim origin in Unreal Engine coordinates. This transformation ensures that UAV states, UGV states, relative poses, and cooperation metrics are evaluated in the same metric frame.

Algorithm 1 summarizes the per-tick execution flow: ground and aerial commands are applied to the shared world, physics is advanced once, and UAV/UGV sensors are sampled from the same updated state. Rendering is forced to complete within the same tick via `FlushRenderingCommands()`, so all sensor outputs are computed from a single physics state before the tick returns.

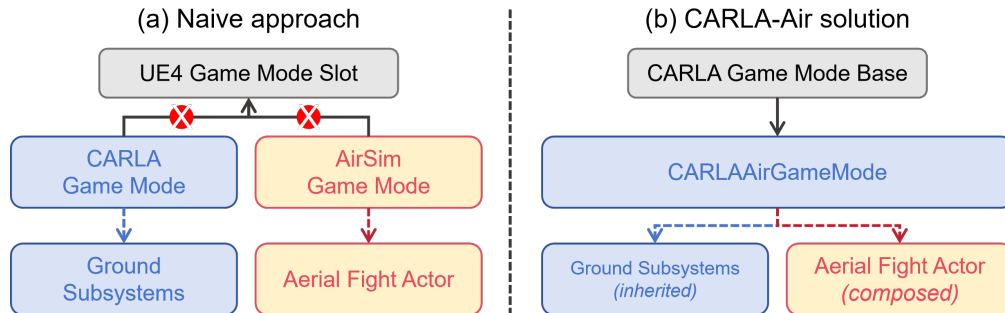


Figure 4: **Resolving the single-GameMode constraint.** A naive merge of CARLA and AirSim creates competing Unreal Engine GameMode controllers. CARLA-AIR preserves CARLA as the authoritative world manager through `CARLAAirGameMode` and composes the AirSim flight actor as a regular world entity, enabling single-process air-ground simulation without competing runtime controllers.

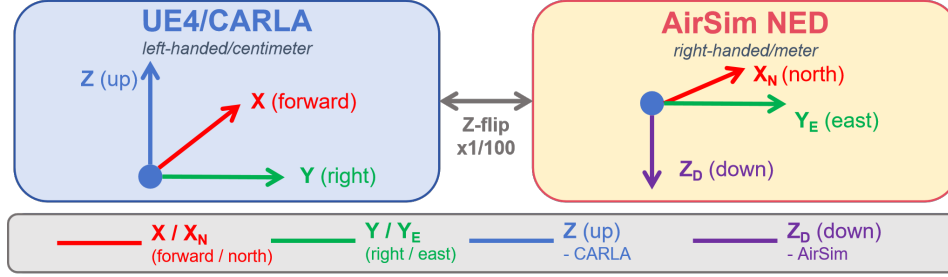


Figure 5: **Coordinate-frame alignment.** CARLA uses the Unreal Engine frame in centimetres with Z -up, while AirSim uses a metre-scale NED frame with Z -down. CARLA-AIR applies a deterministic scale conversion and Z -axis sign flip to express UAV and UGV states in one metric frame.

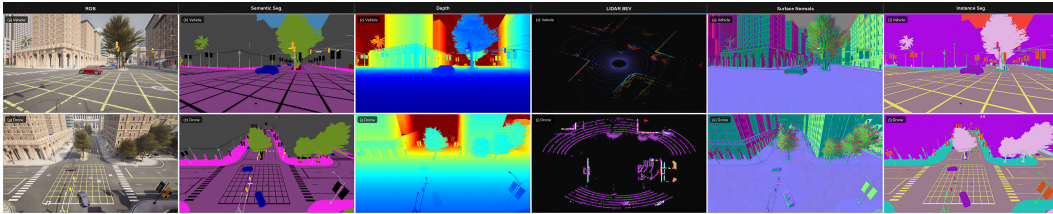


Figure 6: **Example of synchronized aerial-ground sensing.** Vehicle-side and UAV-side sensor streams are sampled from the same simulation tick in CARLA-AIR. The top row shows vehicle-side modalities and the bottom row shows UAV-side modalities, including RGB, semantic segmentation, depth, LiDAR BEV, surface normals, and instance segmentation. This provides paired multi-modal observations without cross-process timestamp alignment.

Algorithm 1 Single-tick execution in CARLA-AIR

- Require:** World state \mathcal{W}_t , UGV action a_t^G , UAV action a_t^A
Ensure: Updated world \mathcal{W}_{t+1} , synchronized observations o_{t+1}^G, o_{t+1}^A
- 1: Apply UGV command a_t^G through the CARLA control interface
 - 2: Apply UAV command a_t^A through the AirSim control interface
 - 3: $\mathcal{W}_{t+1} \leftarrow \text{PHYSICSSTEP}(\mathcal{W}_t)$
 - 4: Render and sample sensors from \mathcal{W}_{t+1}
 - 5: $o_{t+1}^G \leftarrow \text{SAMPLESENSORS}(\text{UGV}, \mathcal{W}_{t+1})$
 - 6: $o_{t+1}^A \leftarrow \text{SAMPLESENSORS}(\text{UAV}, \mathcal{W}_{t+1})$
 - 7: **return** $\mathcal{W}_{t+1}, o_{t+1}^G, o_{t+1}^A$
-

A.2 Sensors and Native APIs

Table 7 lists the sensor modalities supported by CARLA-AIR. All enabled sensors are sampled at the shared simulation tick, so cross-agent correspondence does not require interpolation or extrapolation. CARLA and AirSim retain their original Python APIs and ROS 2 interfaces; both command streams are resolved inside the same Unreal Engine runtime, so existing client code continues to operate without modification. Figure 6 visualizes this same-tick aerial-ground sensing setup.

A.3 Software and Hardware

Table 8 summarizes the software stack used in our experiments. All builds and experiments are run on a single workstation with an Intel Core Ultra 9 275HX (24C/24T) CPU, an NVIDIA RTX 5090 Laptop GPU (24 GB), and 128 GB RAM under Ubuntu 22.04. Runtime evaluation requires a GPU with sufficient memory for the selected VLA baseline.

Table 7: Sensor modalities available in CARLA-AIR. UGV and UAV columns indicate availability on each platform.

#	Sensor	UGV	UAV
1	RGB camera (forward)	✓	✓
2	RGB camera (downward)	—	✓
3	RGB camera (wide-angle)	✓	✓
4	Depth camera	✓	✓
5	Semantic segmentation camera	✓	✓
6	Instance segmentation camera	✓	✓
7	Surface normal camera	✓	✓
8	LiDAR	✓	✓
9	Radar	✓	—
10	IMU	✓	✓
11	GNSS	✓	✓
12	Barometer	—	✓
13	Magnetometer	—	✓
14	Optical flow camera	✓	✓
15	Event camera	✓	✓
16	Collision sensor	✓	✓
17	Lane invasion sensor	✓	—
18	Obstacle distance sensor	✓	✓

Table 8: Software stack used in our experiments.

Component	Version
Unreal Engine	4.26.2
CARLA	0.9.16
AirSim	1.7.0
Python	3.8.18
PyTorch	2.1.2 (CUDA 11.8)
ROS 2	Humble Hawksbill
Ubuntu	22.04 LTS

Note on AirSim. The original open-source AirSim project is no longer actively maintained by Microsoft. We build on Colosseum [32], a community-maintained fork that preserves the AirSim API surface and remains compatible with Unreal Engine.

A.4 Runtime Consistency Validation

This section provides the experimental details underlying the runtime consistency check reported in Section 3.2 (Table 2), and extends the validation to additional sensor configurations, control frequencies, and agent counts.

Setup. The UGV drives along a predefined route in Town10 at constant speed, while the UAV is driven by a position P-controller to follow the UGV at a fixed relative offset; the underlying flight control uses AirSim’s built-in cascaded PID module (the AirSim default configuration [22]).

Comparison configurations. Under the bridge runtime, CARLA and AirSim run as separate processes and exchange messages via ROS 2 at 10 Hz—the architecture commonly used by prior air-ground integrations [3]. Under the CARLA-AIR runtime, both simulators share a single simulation tick. Both runtimes execute the same 100 episodes with matched random seeds, identical spawn points, and the same follow controller; the only varied factor is the runtime architecture.

Measurements. *Sensor offset* is the per-tick timestamp difference $|\tau_{\text{UAV}} - \tau_{\text{UGV}}|$ (ms) between matched UAV and UGV sensor frames. *Follow-error std* is the per-episode mean of the Euclidean

Table 9: **Runtime stress test.** Bridge timestamp offset (mean/P95, ms), wall-clock delivery jitter (P95, ms), and metric noise reduction (σ ratio = bridge / CARLA-AIR cooperation-metric std, mean \pm std over 5 independent 100-episode runs). CARLA-AIR maintains zero simulation-timestamp offset in all settings.

Setting (agents, sensors, Hz)	Bridge offset mean/P95 (ms)	CARLA-AIR offset (ms)	WC jitter P95 (ms)	σ ratio
Easy-RGB (1U+1G, RGB, 10 Hz)	12.4/34	0.0	4	$5.1 \pm 0.4 \times$
Multi-sensor (1U+1G, RGB+D+L, 10 Hz)	15.2/41	0.0	7	$4.8 \pm 0.4 \times$
High-rate (1U+1G, RGB, 30 Hz)	18.7/52	0.0	9	$6.3 \pm 0.5 \times$
Multi-agent (2U+2G, RGB+L, 10 Hz)	22.1/64	0.0	12	$4.2 \pm 0.4 \times$
Dense-traffic (1U+1G, RGB, 10 Hz)	13.1/37	0.0	5	$5.0 \pm 0.4 \times$

distance (in metres) between the UAV’s actual relative pose and its target relative pose during the steady-state segment of the episode, taken as the standard deviation across the 100 episodes; this is the σ reported in Table 2. *Wall-clock jitter* (used in Table 9) is the standard deviation of OS frame-delivery timestamps after the physics tick returns, and arises from GPU flush overhead. The reported $5.1 \times$ noise reduction has a 95% confidence interval of $[3.4 \times, 7.7 \times]$ (F-distribution, $n_1 = n_2 = 100$).

Stress-test extension. Table 9 extends this protocol to heavier sensor payloads, higher control rates, multi-agent settings, and dense traffic. CARLA-AIR maintains $\Delta t = 0$ ms by construction in all configurations, with σ ratios in the $4.2 \times - 6.3 \times$ range; remaining wall-clock jitter (4–12 ms P95) is substantially lower than bridge timing noise.

A.5 Source Modification Summary

The CARLA-AIR integration modifies only a small number of files relative to the CARLA upstream codebase:

- `CarlaUE4GameMode.h`: adds the AirSim flight actor declaration and composition pointer.
- `CarlaUE4GameMode.cpp`: instantiates the AirSim actor and synchronizes it with the CARLA world lifecycle.
- `CarlaUE4.Build.cs`: adds the AirSim module dependency.

The integration preserves the native CARLA and AirSim client-facing APIs.

B Additional Diagnostic Evaluation Details

This appendix provides details omitted from the main diagnostic evaluation section, including task settings, cooperation modes, prompt templates, metric definitions, baseline adaptations, and evaluation protocol.

B.1 Task Details

Cooperative Moving-Platform Landing. A UGV truck drives along an urban road while providing a flat rear cargo bed as the landing surface. The UAV receives the instruction: *Follow the moving truck, align above its rear cargo bed, and land safely.* The task consists of tracking, alignment, and landing, with a 60 s episode time limit. It is successful only when the UAV lands on the rear cargo bed without collision, side impact, or hard landing.

Cooperative Occlusion-Recovery Escort. A UGV drives along an urban route and becomes temporarily occluded by bridges, buildings, or large artifacts. The UAV must escort the UGV and recover visual contact after the target becomes invisible. Each escort episode has a 90 s time limit. The C1 cue describes the UGV’s motion intent and expected reappearance direction, while the VLA policy still outputs only UAV actions.

B.2 Cooperation Modes

C0: Independent execution. The UAV and UGV do not communicate. The UGV follows a predefined speed profile or route, while the UAV relies only on onboard RGB observations and the task instruction.

C1: UGV-to-UAV semantic prompting. The UGV provides a compact semantic cue to the UAV. For landing, the cue describes the relative direction to the cargo bed, coarse truck motion, and landing phase. For occlusion recovery, it describes the occlusion status, motion intent, and expected reappearance direction. The UAV still outputs only native UAV actions.

C2: Bidirectional UAV-to-UGV action coupling. C2 is used only for Moving-Platform Landing. The UAV receives the same semantic cue as in C1. The magnitude of the UAV’s commanded forward velocity is passed directly to a fixed UGV longitudinal controller, with no intermediate phase decoder or learned mapping:

$$v_{\text{UGV}}(t) = v_0 \cdot \text{clip}\left(\frac{\|v_{\text{UAV}}^{\text{fwd}}(t)\|}{v_{\text{ref}}}, 0.5, 1.5\right), \quad (2)$$

where $v_0 = 4.0\text{ m/s}$ is the nominal UGV speed and $v_{\text{ref}} = 2.0\text{ m/s}$ is a reference scaling constant. The $\text{clip}(\cdot, 0.5, 1.5)$ operator bounds the multiplicative factor to $[0.5\times, 1.5\times]$ to prevent extreme values. The controller modulates only longitudinal speed; the UGV heading and route remain unchanged. The update frequency matches the UAV decision frequency. For baselines whose native output is not a continuous velocity vector (OpenFly, AerialVLN), $\|v_{\text{UAV}}^{\text{fwd}}(t)\|$ is obtained from the realized UAV forward velocity in the simulator at the same tick. For waypoint-output baselines (SPF, OpenUAV), it is computed as commanded waypoint displacement divided by the inference period. The updated UGV state is then fed back to the UAV prompt for the next step. No additional VLA output head or UGV steering command is introduced; the protocol is intentionally a naive form of bidirectional action coupling.

B.3 Prompt Templates

Table 10 lists the full prompt templates used across tasks and cooperation modes. All VLA baselines receive the same base instruction within each task, with mode-specific assistant hints appended for C1 and C2.

B.4 Metric Details

Tracking Success Rate. Tracking Success Rate (TSR) measures whether the target truck remains inside the UAV camera view for at least $K = 3\text{ s}$ of cumulative time before task termination. It evaluates the single-UAV tracking primitive rather than final task success.

Landing Success Rate. Landing Success Rate (LSR) measures the fraction of episodes in which the UAV lands on the rear cargo bed within the 60 s time limit and remains stable after touchdown, defined as no further displacement exceeding 0.3 m within 2 s of first contact.

Cooperative Conversion Rate. Cooperative Conversion Rate (CCR) measures whether single-UAV tracking becomes cooperative landing:

$$\text{CCR} = \frac{\text{LSR}}{\max(\text{TSR}, \varepsilon)}.$$

We set $\varepsilon = 0.05$; substituting $\varepsilon \in \{0.01, 0.05, 0.10\}$ changes CCR by at most 0.01 across all reported conditions, as all baselines achieve $\text{TSR} \geq 0.55$ under C0. A high TSR with low CCR indicates that the UAV can track the moving platform but cannot convert tracking into landing.

Cooperation Gain. Cooperation Gain (CG) measures the change in LSR relative to independent execution:

$$\text{CG}(C_k) = \text{LSR}(C_k) - \text{LSR}(C_0).$$

Positive CG means that the cooperation mode improves over C0, while negative CG indicates degradation.

Table 10: **Full prompt protocol.** All VLA baselines receive the same base instruction within each task. C1 uses semantic partner-state prompts. C2 uses the same UAV-side prompt as C1 and only enables the UGV-side longitudinal response to UAV action.

Task	Mode	Interaction	UAV prompt example
Landing	C0	No communication	<i>Follow the moving truck, keep it in view, align above the flat rear cargo bed, and land safely on the cargo bed.</i>
Landing	C1	Semantic state cue	<i>Follow the moving truck, keep it in view, align above the flat rear cargo bed, and land safely on the cargo bed. Assistant hint: the cargo bed is forward-left. The truck is moving slowly. Current phase: approach. Use the hint only to choose your next UAV action.</i>
Landing	C2	Same UAV prompt as C1; UGV speed responds to UAV forward velocity	<i>Follow the moving truck, keep it in view, align above the flat rear cargo bed, and land safely on the cargo bed. Assistant hint: the cargo bed is forward-left. The truck is moving slowly. Current phase: approach. Use the hint only to choose your next UAV action.</i>
Escort	C0	No communication	<i>Follow the moving truck and keep it in view.</i>
Escort	C1	Occlusion-recovery cue	<i>Follow the moving truck and keep it in view. Assistant hint: the truck is temporarily occluded by the bridge. The truck continues forward and will reappear on the forward-right side. Current phase: occlusion recovery. Use the hint only to recover visual contact.</i>
Landing	C1-Oracle-Bearing	Oracle geometric cue	<i>Follow the moving truck, keep it in view, align above the flat rear cargo bed, and land safely. State update: cargo bed at bearing 312°, range 6.2 m, elevation -8°. Phase: approach. Use the state update only to choose your next UAV action.</i>

Occlusion-recovery metrics. Recovery Success Rate (RSR) measures whether the UAV recovers visual contact with the UGV within 15 s of occlusion onset; success requires $\text{IoU} \geq 0.15$ between the UAV camera view and the UGV bounding box, sustained for at least 0.5 s. Re-acquisition Time (RAT) is measured from occlusion onset to the first frame satisfying the IoU threshold; it is capped at 15 s for episodes with no recovery. Each escort episode contains 1–3 occlusion events sampled from three geometry types (bridge underpass: 40%, building: 35%, large artifacts: 25%), with occlusion duration drawn uniformly from 4–12 s.

Timing metrics. Decision Frequency (DF) is the realized control update rate of each aerial policy. Effective Coordination Latency (ECL) measures the delay from a newly generated UAV action or UGV state update to its use by the partner side in the next control step.

Statistical analysis. All values are reported as mean \pm std over 3 seeds \times 50 episodes per condition. Across-baseline trends are tested with a sign test on per-seed-mean CGs ($n=5$ baselines). Single-baseline 95% confidence intervals are computed via hierarchical bootstrap clustered by seed (1000 resamples) to account for episode dependencies within seeds.

B.5 Baseline Adaptation Details

Table 11 summarizes how each baseline is adapted to the CARLA-AIR evaluation interface. All baselines use officially released checkpoints without fine-tuning or task-specific training.

AerialVLA. AerialVLA is an end-to-end aerial VLA policy outputting continuous UAV velocity commands directly from onboard visual observations and language instructions. Its native UAV-action interface is kept unchanged; cooperation is introduced only through the C0/C1/C2 protocols.

Table 11: **Baseline adaptation summary.** All methods use official checkpoints without fine-tuning. Heterogeneous low-level wrappers preserve each baseline’s native operating regime; comparisons reflect policy family characteristics rather than implementation-matched rankings. DF: realized decision frequency under evaluation conditions.

Method	Original task	Native output	Action mapping	Controller	DF (Hz)
AerialVLA	UAV nav. + VLA	UAV velocity cmd	Direct passthrough; task prompt rewritten for landing/escort	AirSim cmd passthrough	6.2
OpenFly	Aerial VLN + VLA	Discrete UAV action	{Forward 3/6/9 m, Turn left/right, Up, Down, Stop} mapped to fixed-duration velocity bursts	Fixed-duration AirSim cmd	3.1
OpenUAV	UAV traj. generation	Dense traj. array	1 s segment sampled at 10 Hz; replanned every 0.6 s	AirSim velocity controller	1.6
SPF	UAV way-point nav.	Single waypoint	One waypoint per inference; position controller tracks it	AirSim position ctrl ($K_p=0.8$)	1.1
AerialVLN	Language-cond. UAV nav.	Discrete UAV cmd	{forward, left, right, up, down, hover} mapped to 0.5 s velocity bursts at 1.5 m/s	Fixed-duration AirSim cmd	9.0
Rule-Coop-State	Designed for this eval	UAV + UGV cmd pair	Direct metric-state feedback for UGV side)	State-feedback rule	50+

OpenFly. OpenFly is a keyframe-aware aerial VLA model fine-tuned from OpenVLA-7B on the OpenFly aerial VLN dataset [5]. Its native output is a discrete action vocabulary {Forward 3/6/9m, Turn left, Turn right, Up, Down, Stop}, which we map to fixed-duration velocity bursts in CARLA-AIR following the same adaptation pattern used for AerialVLN. Cooperation is introduced only through the C0/C1/C2 protocols.

OpenUAV. OpenUAV is an end-to-end aerial VLA model that generates a continuous UAV trajectory via MLLM-based planning. The first 1 s segment of the trajectory is passed to the AirSim velocity controller, and the trajectory is replanned every 0.6 s.

SPF. SPF uses explicit spatial reasoning via a VLM planner and outputs a single waypoint per inference. The waypoint is tracked by a position controller.

AerialVLN. AerialVLN is a pre-LLM cross-modal aerial navigation baseline. Its discrete action vocabulary is mapped to fixed-duration velocity bursts in CARLA-AIR.

Rule-Coop-State. Rule-Coop-State uses explicit metric state (UAV–cargo-bed relative pose, relative velocity, UGV speed, landing phase) and applies deterministic low-latency rules for UAV descent and UGV longitudinal speed adjustment (see Section 4.2 for framing).

B.6 Prompt-Format Ablation

Table 12 shows the C1 prompt variants used in the prompt-format ablation. The base task instruction remains unchanged within each task; only the appended assistant hint is modified. C1-Sem is the default semantic partner-state cue used in the main evaluation. C1-Num uses structured numeric state fields. C1-Noisy corrupts direction, motion, or phase fields. C1-Oracle-Bearing replaces the semantic hint with ground-truth geometric bearing, range, and elevation while keeping the native UAV action interface unchanged.

Table 12: **Prompt variants for C1 ablation.** Examples show the assistant hint appended to the unchanged base task instruction. Landing variants provide cargo-bed state, while escort variants provide occlusion-recovery and expected reappearance state.

Task	Variant	State format	Assistant hint example
Landing	C1-Sem	Semantic	<i>Assistant hint: the cargo bed is forward-left. The truck is moving slowly. Current phase: approach. Use the hint only to choose your next UAV action.</i>
Landing	C1-Num	Numeric	<i>State: truck speed = 2.0 m/s; truck heading = 15 deg; relative bearing to cargo bed = -30 deg; relative distance to cargo bed = 8.0 m; phase = approach.</i>
Landing	C1-Noisy	Corrupted semantic	<i>Assistant hint: the cargo bed is right. The truck is nearly stopped. Current phase: descend. Use the hint only to choose your next UAV action.</i>
Landing	C1-Oracle-Bearing	Oracle geometry	<i>State update: cargo bed at bearing 312°, range 6.2 m, elevation -8°. Phase: approach. Use the state update only to choose your next UAV action.</i>
Escort	C1-Sem	Semantic	<i>Assistant hint: the truck is temporarily occluded by the bridge. The truck continues forward and will reappear on the forward-right side. Current phase: occlusion recovery. Use the hint only to recover visual contact.</i>
Escort	C1-Num	Numeric	<i>State: occlusion = true; truck speed = 2.0 m/s; expected reappearance bearing = 35 deg; expected reappearance distance = 9.4 m; phase = occlusion recovery.</i>
Escort	C1-Noisy	Corrupted semantic	<i>Assistant hint: the truck is temporarily occluded. The truck will reappear on the rear-left side. Current phase: normal escort. Use the hint only to recover visual contact.</i>
Escort	C1-Oracle-Bearing	Oracle geometry	<i>State update: UGV at bearing 35°, range 9.4 m, elevation -12°. Phase: occlusion recovery. Use the state update only to recover visual contact.</i>

Table 13: **Timing statistics.** DF: realized decision frequency (Hz). ECL (Effective Coordination Latency): delay from policy inference completion to partner-side controller consumption; excludes UAV actuator delay. Values are episode-level medians with IQR (P25–P75) over 50 episodes per method.

Method	DF (Hz)↑	ECL mean (ms)↓	ECL P95 (ms)↓	ECL IQR (ms)
AerialVLA	6.2	160	260	120–190
OpenFly	3.1	330	520	240–400
OpenUAV	1.6	620	950	450–740
SPF	1.1	850	1250	620–1050
AerialVLN	9.0	110	180	80–135
Rule-Coop-State	50+	20	35	15–25

B.7 Evaluation Protocol

Unless otherwise specified, each method is evaluated under the same route, spawn, weather, and random-seed protocol within each diagnostic task. The UGV route and speed profile are fixed for C0 and C1. In C2, only the UGV longitudinal speed is adjusted by the fixed response controller; the route is unchanged. All VLA policies receive the same task instruction and the same mode-specific prompt template.